ChemComm



COMMUNICATION

View Article Online



Cite this: Chem. Commun., 2021. **57**, 7264

Received 21st April 2021, Accepted 24th June 2021

DOI: 10.1039/d1cc02114a

rsc.li/chemcomm

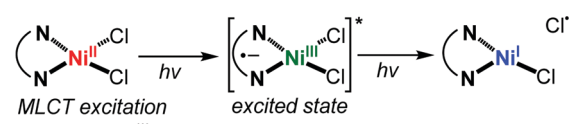
Photoreductive chlorine elimination from a Ni(III)Cl₂ complex supported by a tetradentate pyridinophane ligand†

Hanah Na, Da Michael B. Watson, Fengzhi Tang, Nigam P. Rath and Liviu M. Mirica 🗅 *a

Herein we report the isolation, characterization, and photoreactivity of a stable Ni^{III} dichloride complex supported by a tetradentate pyridinophane N-donor ligand. Upon irradiation, this complex undergoes an efficient photoreductive chlorine elimination reaction, both in solution and the solid-state. Subsequently, the Ni^{III}Cl₂ species can be regenerated via a reaction with PhICl₂.

Photoreductive halogen elimination reactions are of growing interest due to their relevance to the photodriven HX-splitting reactions, which have been considered promising chemical strategies for solar-to-fuel energy conversion. 1-4 Most commonly, precious 2nd and 3rd row transition metal complexes of Ir, Au, or Rh are exploited for this type of reaction due to their favorable photophysical and photochemical properties. 5-10 However, for a sustainable system, it is imperative to replace precious metal ions with earth-abundant 1st row metal ions. 11,12 Recent work from Nocera et al. demonstrated efficient halogen elimination photoreactions from Ni^{III} trihalide complexes supported by bidentate phosphine ligands. 13,14 The targeted design strategy is inspired by the seminal work of Hillhouse, where reductive elimination from a Ni^{III} state is preferred over a $\mathrm{Ni^{II}}$ state. $^{15-18}$ Instead of accessing a $\mathrm{Ni^{III}}$ -like state via excitation of Ni^{II} species into the metal-to-ligand charge transfer (MLCT) state, starting with a Ni^{III} complex would circumvent the inherent drawback of short excitedstate lifetimes for the 1st row transition metal complexes (Scheme 1).19 More recently, Castellano et al. showed visible light-induced Cu-Cl homolytic bond cleavage reaction in [Cu(dmp)₂Cl]⁺. ²⁰ Nevertheless, beyond the above examples little

Our group has employed the tetradentate N-donor ligands N,N-dialkyl-2,11-diaza[3.3](2,6)pyridinophane ($^{R}N4$, R = Me, iPr, tBu) to stabilize various mononuclear high-valent Ni complexes and investigate their C-C/C-heteroatom bond formation reactivity. 25-29 Accordingly, we postulated that this ligand system could be exploited to stabilize NiIII dihalide species, and therefore allow us to investigate their photoreactivity. Herein, we report the isolation, characterization, and photoreactivity



accessing Ni^{III}-like state

not efficient due to the short lifetime of Ni^{III}-like excited state

$$\begin{pmatrix}
\mathbf{N} & \mathbf{N}i & \mathbf{C}I \\
\mathbf{N} & \mathbf{N}i & \mathbf{C}I
\end{pmatrix}$$

$$\begin{pmatrix}
\mathbf{N} & \mathbf{N}i & \mathbf{C}I \\
\mathbf{N} & \mathbf{N}i & \mathbf{C}I
\end{pmatrix}$$

$$\begin{pmatrix}
\mathbf{N} & \mathbf{N}i & \mathbf{C}I \\
\mathbf{N} & \mathbf{N}i & \mathbf{C}I
\end{pmatrix}$$

$$\begin{pmatrix}
\mathbf{N} & \mathbf{N}i & \mathbf{C}I \\
\mathbf{N} & \mathbf{N}i & \mathbf{C}I
\end{pmatrix}$$

$$\begin{pmatrix}
\mathbf{N} & \mathbf{N}i & \mathbf{C}I \\
\mathbf{N} & \mathbf{N}i & \mathbf{C}I
\end{pmatrix}$$

$$\begin{pmatrix}
\mathbf{N} & \mathbf{N}i & \mathbf{C}I \\
\mathbf{N} & \mathbf{N}i & \mathbf{C}I
\end{pmatrix}$$

starting from Ni^{III} circumvents short-lived Ni^{III}-like excited state

Scheme 1 Strategies for the photoreductive chlorine elimination from Ni complexes.

progress has been made toward a photoreductive halide elimination reaction from other 1st row transition metal complexes, and therefore more diverse molecular platforms that support such a reaction need to be identified. We note that photoelimination reactivity examples of Ni^{III} complexes supported by N-donor ligands are very rare, partially due to the instability of these complexes that prevents their detailed characterization. In recent years, photocatalytic generation of chlorine radicals from (bpy)-Ni^{III} complexes and their use in photoredox cross-coupling catalysis has been reported by Doyle et al. and Molander et al. 21-24 Despite the prevalence of chlorine photoelimination reaction from high-valent Ni species in these proposed mechanisms, little is known about their photophysics and photochemistry. This emphasizes the need to investigate the photoreactivity of isolated high-valent Ni complexes supported by N-donor ligands.

^b Department of Chemistry, Washington University, St. Louis, Missouri, 63130, USA ^c Department of Chemistry, University of Missouri-St. Louis, St. Louis, Missouri, 63121. USA

[†] Electronic supplementary information (ESI) available: Experimental and computational details, cyclic voltammograms, and X-ray crystallographic data. CCDC 2076279 (1⁺) and 2076280 (2⁺). For ESI and crystallographic data in CIF or other electronic format see DOI: 10.1039/d1cc02114a

Communication ChemComm

Fig. 1 Synthesis of MeN4Ni^{II}Cl₂ (1) and [MeN4Ni^{III}Cl₂]⁺ (1⁺) complexes and ORTEP representation of the cation of [1]PF₆. Ellipsoids are shown at 50% probability level, with hydrogen atoms, counterion and an outer-sphere solvent molecule eliminated for clarity. Selected bond lengths (Å): Ni1-N1 1.900(3), Ni-N2 1.869(9), Ni-N3 2.159(3), Ni-N4 2.159(3), Ni-Cl1 2.2138(9), Ni-Cl2 2.1885(9).

study of a stable Ni^{III} dichloride complex supported by the tetradentate pyridinophane ligand MeN4, [MeN4Ni^{III}Cl₂]⁺ (1⁺). Although several N-donor supported Ni^{III} monochloride species, 30,31 porphyrin NiIII dibromide complexes, 32 and mixed N/C-donor supported Ni^{III} halide complexes^{27,33–39} were reported, none of them were studied in terms of their photochemistry. To the best of our knowledge, 1⁺ represents the first isolated all N-donor supported Ni^{III} chloride complex for which its photochemistry was investigated.

The green complex MeN4Ni^{II}Cl₂ (1) was prepared by stirring MeN4 and Ni(DME)Cl₂ in CH₂Cl₂ overnight (Fig. 1).²⁸ The cyclic voltammetry (CV) of 1 exhibits a pseudo-reversible oxidation wave at 0.52 V νs . Fc^{+/0}, followed by an irreversible oxidation at 0.97 V vs. $Fc^{+/0}$ (Fig. S1, ESI†). The first oxidation wave is assigned to the Ni^{III}/Ni^{II} couple and this oxidation potential is similar to the reported value of Ni^{III}/Ni^{II} couple for ^{tBu}N4NiCl₂ of 0.52 V vs. Fc+/0, indicating a minimal effect of the axial N-substituents. 40 As the oxidation potential is chemically accessible, complex 1 can be easily oxidized with 1 equiv. thianthrenyl tetrafluoroborate, resulting in $[MeN4Ni^{III}Cl_2]BF_4$ ([1]BF₄) and as evidenced by an immediate color change from light green to dark purple. The effective magnetic moment μ_{eff} of 2.13 μ_{b} , determined using the ¹H NMR Evans method, is consistent with an S = 1/2 ground state for $\mathbf{1}^+$, as expected for a Ni^{III} center. 41,42 Interestingly, 1 was stable at room temperature as a solid or in solution, showing minimal decomposition unless it was exposed to water (Fig. S3, ESI†), unlike other known N-donor supported Ni^{III} mono or dichloride complexes that exhibit limited stability in solution at room temperature. 30,31,40 Single crystals of [1]PF6 suitable for X-ray diffraction were grown via the diffusion of pentane into a CH₂Cl₂ solution of the complex. The complex [1]PF₆ shows the presence of a Ni^{III} center that adopts a distorted octahedral geometry, with coordination to two pyridines and two amines of the MeN4 ligand (Fig. 1). The average axial Ni-Nax bond distance (2.159 Å) is substantially longer than the equatorial Ni-N_{eq} bond distance (1.885 Å). The average Ni-Cl bond length (2.201 Å) is similar to those of pincer-type Ni^{III} chloride species (2.286 or 2.276 Å)^{34,37} or the Ni^{III} complexes supported by phosphine ligands (2.219-2.287 Å). 13,14 The density functional theory (DFT) optimized geometry of 1⁺ exhibits a slightly longer average bond lengths (Ni-N_{eq} 1.9247 Å, Ni-N_{ax} 2.2199 Å, Ni-Cl 2.2438 Å) but overall they are in good agreement with the experimental values. The EPR spectrum of 1⁺ exhibits a pseudoaxial signal with g_x , g_y , and g_z values of 2.149, 2.149, and 2.027, respectively (Fig. 2a). Superhyperfine coupling to the two axial nitrogen atoms (I = 1), primarily in the g_z direction ($A_{2N} =$ 18.5 G) was observed, consistent with formation of d⁷ Ni^{III} species with a S = 1/2 ground state in which the unpaired electron occupies primarily the d_z^2 orbital of the Ni center. ^{43–46} Additionally, the DFT calculated spin density supports a metalbased radical description for $\mathbf{1}^+$, and the predominant d_z^2 character of the unpaired electron (Fig. 2b). The UV-visible absorption spectra of 1 and 1⁺ were obtained in MeCN (Fig. S7, ESI†). The absorption spectrum of Ni^{II} complex 1 is dominated by a band at 371 nm (ε = 328 M⁻¹ cm⁻¹) and a much weaker band at 600 nm (ε = 20 M⁻¹ cm⁻¹). On the other hand, the Ni^{III} complex 1+ exhibits a more intense band at 354 nm $(\varepsilon = 1948 \text{ M}^{-1} \text{ cm}^{-1})$ and a low-energy absorption band at 563 nm (ε = 211 M⁻¹ cm⁻¹). To probe the nature of the electronic transitions, time-dependent density functional theory (TD-DFT) calculations of 1⁺ were performed using the B3LYP functional and the 6-31G* basis set. The simulated absorption spectrum matched closely with the experimental result (Fig. 3). According to the calculations, the transitions in the blue region (400-500 nm) involve excited states that arise from the population of the LUMOs possessing Ni–Cl σ^* character (Fig. S23–S25, ESI†).⁴⁷ Natural transition orbitals (NTOs) analysis (Fig. 3, inset), which visualizes a localized picture of the transition density matrix, 48 confirms the assignment of the bands between 400 nm and 600 nm to ligand-to-metal charge transfer (LMCT) transitions, corresponding to the promotion of an electron from orbitals primarily localized on the MeN4 ligand and/or the Cl ligand to the Ni-Cl antibonding MOs. The lower energy absorption bands over 600 nm correspond to primarily

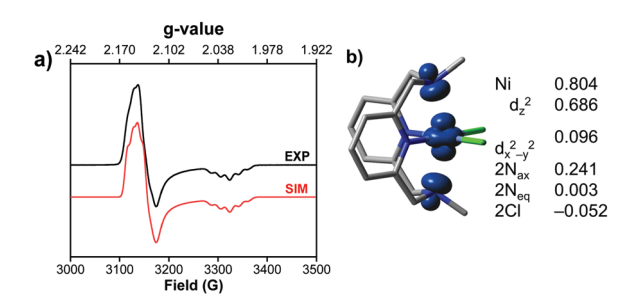


Fig. 2 (a) Experimental (1:3 MeCN: PrCN, 77 K) and simulated EPR spectra of $\mathbf{1}^+$ using the following parameters: $g_x = 2.149$, $g_y = 2.149$, $g_z = 2.027$, $A_x(2N) = 12$ G, $A_y(2N) = 12$ G, $A_z(2N) = 18.5$ G. (b) DFT calculated Mulliken spin density for 1^+ (shown as a 0.05 isodensity contour plot).

ChemComm Communication

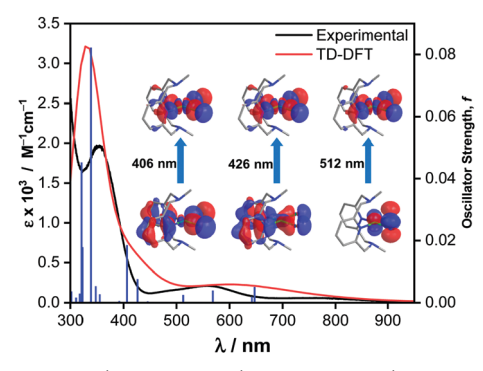


Fig. 3 Experimental (black solid line) and calculated (red solid line) UV-vis absorption spectra of ${f 1}^+$ overlaid with oscillator (blue solid bars). Inset: The NTOs for the transitions associated with blue light (400–500 nm) excitation.

d–d transitions (Fig. S27 and S28, ESI \dagger). Overall, based on the TD-DFT calculations, excitation of the LMCT bands of $\mathbf{1}^{\dagger}$ with blue LED irradiation is proposed to induce photoreduction of the complex with concurrent Ni–Cl bond dissociation.

In agreement with this spectroscopic assignment, irradiation of a MeCN solution of $\mathbf{1}^+$ with blue LED ($\lambda_{\rm max}=456$ nm) resulted in a rapid quenching of the band at 563 nm, suggesting a facile photoreduction of the Ni^{III} complex (Fig. 5), while 1 did not display a significant spectral change over a longer time span (Fig. S8, ESI†). No olefinic traps were required to promote halogen elimination, and Cl-based products were not detected. This is reminiscent of the photoreactivity of the phosphine–Ni^{III} trichloride complexes, where the photo-eliminated chloride is trapped via H atom abstraction from the solvent. 13,14,30 The quantum yield ($\Phi_{\rm p}$) of halogen elimination from 1 $^+$ was determined to be 47% in MeCN, using potassium ferrioxalate as a chemical actinometer. The obtained quantum yield is comparable to the values for the phosphine-supported Ni^{III} trichloride complexes, which range from 13% to 96%. 13,14

The photoreduction reaction was also monitored by paramagnetic ¹H NMR (Fig. S11, ESI†), and a comparison of the ¹H NMR spectra with the independently synthesized Ni^{II} complexes identified the photoreduced product as the monosolvento complex [MeN4Ni^{II}Cl(MeCN)] (2⁺), which was formed in 89% yield (Fig. S12, ESI†). The complex 2⁺ can be synthesized independently through chloride abstraction with KPF₆ from 1 in MeCN, and the structure of 2+ was confirmed by singlecrystal X-ray diffraction, albeit the MeOH analogue was characterized since diffraction-quality crystals could only be obtained in the presence of MeOH (Fig. 4). Overall, an elongation of all Ni–X bond distances (X = N or Cl) compared to those of 1⁺ was observed, due to the presence of a reduced Ni center. The average Ni-N_{eq} distance (2.024 Å) and Ni-Cl bond distance (2.361 Å) are significantly elongated (by ~ 0.160 Å), while the average Ni-Nax bond distance (2.193 Å) is only marginally increased (by 0.034 Å) vs. those in 1⁺. Importantly, the addition of PhICl₂ into the solution of photogenerated 2⁺ (i.e., the irradiated solution of 1⁺) led to an enhancement of the absorption band at 560 nm (Fig. S13, ESI†) and a color change to dark purple, which supports the regeneration of 1⁺. Finally, the solid-state photoreduction of 1+ was also tested, and irradiation

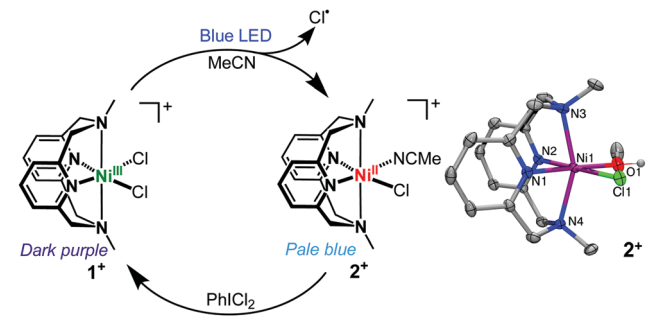


Fig. 4 (left) Photolysis of $\mathbf{1}^+$ affording photoreduced Ni^{II} complex $\mathbf{2}^+$ and regeneration of $\mathbf{1}^+$ achieved with PhICl₂. (right) ORTEP representation of $\mathbf{2}^+$. Ellipsoids are shown at 50% probability level, with carbon-bound hydrogen atoms, counterion and an outer-sphere solvent molecule eliminated for clarity. Selected bond lengths (Å): Ni1–N1 2.009(3), Ni–N2 2.034(3), Ni–N3 2.197(3), Ni–N4 2.189(3), Ni–Cl1 2.3611(8), Ni–O1 2.065(3).

of solid [1]BF4 showed noticeable signs of discoloration from dark purple to light blue (Fig. S15, ESI†). The evolution of evolved Cl₂ was confirmed qualitatively via the N,N-diethyl-1,4phenylenediamine (DPD) colorimetric method (Fig. S19, ESI†), 13,14 indicating that halide photoelimination from a Ni^{III} complex supported by N-donor ligands can also be promoted in the solid-state. ¹H NMR analysis of the photolyzed solid for 10 h indicated a 67% conversion of 1⁺ into 2⁺ (Fig. S18, ESI[†]). In addition, photolysis of solid [1]BF4 as a suspension in THF was performed with a radical trapping agent, N-tert-butyl-αphenylnitrone (PBN) (Fig. S20, ESI†). The EPR spectrum of the reaction mixture supports the formation of the PBN-THF adduct (g = 2.0061, $A_N = 14.6$ G, $A_H = 3.0$ G, $A_C(THF) = 3.0$ G, $A_{\rm H}({\rm THF}) = 0.90$ G), as the superhyperfine coupling constants of the spin adduct agreed well with reported values (Fig. 6). 49,50 The PBN-THF spin adduct is believed to be formed through H atom abstraction by the photoeliminated chlorine radical and this is reminiscent of the work described by Castellano et al., in which the PBN-THF spin adduct has been detected after Cu-Cl bond cleavage.20

In conclusion, herein we report a Ni^{III} dichloride complex (1⁺) supported by a tetradentate N-donor pyridinophane ligand (MeN4) and its photoinduced halogen elimination reactivity. The MeN4 ligand can successfully stabilize a Ni^{III} dichloride complex 1+, allowing for isolation and detailed investigation of its photochemistry at RT. The titled complex was photoreduced upon blue light excitation, with elimination of chloride in the absence of a chemical trap. Characterization of the photoreduced Ni product, EPR spin trapping, and DPD colorimetric experiments provide strong evidence for the chlorine elimination reaction. TD-DFT calculations suggest that blue light excitation of 1⁺ resulted in population of the LUMOs possessing Ni-Cl σ^* character, corresponding to a photodissociative LMCT state. An important aspect of this work is the isolation, characterization, and photoreactivity study of a high-valent Ni dichloride complexes supported by a multidentate N-donor ligand, that appears to bear no precedent. This work may offer a platform not only for a photocatalytic HX splitting cycle, but also for related photoredox cross-coupling catalytic systems

Communication ChemComm

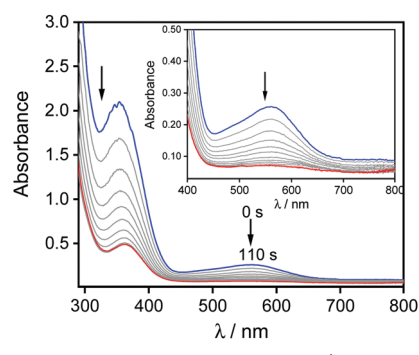


Fig. 5 Photolysis of 1.3 mM MeCN solution of 1⁺ with 456 nm blue LED excitation. The initial spectrum (blue line) converts to that of 2+ (red line) over the course of 110 s. Spectra were recorded every 10 s.

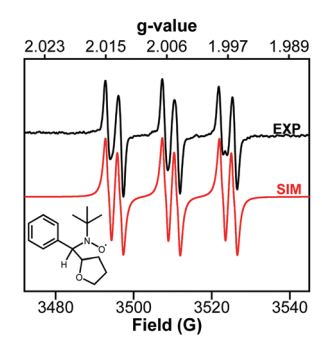


Fig. 6 EPR spectrum of irradiated solid 1+ in the presence of PBN. Parameters used for simulation: g = 2.0061, $A_N = 14.6$ G, $A_H = 3.0$ G, $A_{\rm C}({\rm THF}) = 3.0$ G, $A_{\rm H}({\rm THF}) = 0.90$ G, linewidth 1.15 G.

involving photochemically generated radical species. Current studies are targeting the examination of the photophysics and photochemistry of stable $\lceil (^{R}N4)Ni^{III}ArX \rceil^{+}$ (X = halide) complexes reported by our group,25 which are directly relevant to the commonly proposed photoactive Ni complexes in crosscoupling catalysis.

The authors acknowledge the National Science Foundation (CHE-1925751) for funding.

Conflicts of interest

There are no conflicts to declare.

Notes and references

- 1 A. J. Esswein and D. G. Nocera, Chem. Rev., 2007, 107, 4022.
- 2 D. G. Nocera, Inorg. Chem., 2009, 48, 10001.
- 3 T. S. Teets and D. G. Nocera, Chem. Commun., 2011, 47, 9268.
- 4 L. Troian-Gautier, M. D. Turlington, S. A. M. Wehlin, A. B. Maurer, M. D. Brady, W. B. Swords and G. J. Meyer, Chem. Rev., 2019, 119, 4628.
- 5 T. R. Cook, A. J. Esswein and D. G. Nocera, J. Am. Chem. Soc., 2007, 129, 10094.
- 6 T. R. Cook, Y. Surendranath and D. G. Nocera, J. Am. Chem. Soc., 2009, 131, 28.
- 7 T. S. Teets and D. G. Nocera, J. Am. Chem. Soc., 2009, 131, 7411.
- 8 T. S. Teets, D. A. Lutterman and D. G. Nocera, Inorg. Chem., 2010, 49, 3035.
- 9 H. Yang and F. P. Gabbaï, J. Am. Chem. Soc., 2014, 136, 10866.
- 10 D. C. Powers, M. B. Chambers, T. S. Teets, N. Elgrishi, B. L. Anderson and D. G. Nocera, Chem. Sci., 2013, 4, 2880.

- 11 R. M. Izatt, S. R. Izatt, R. L. Bruening, N. E. Izatt and B. A. Moyer, Chem. Soc. Rev., 2014, 43, 2451.
- 12 C. Förster and K. Heinze, Chem. Soc. Rev., 2020, 49, 1057.
- 13 S. J. Hwang, B. L. Anderson, D. C. Powers, A. G. Maher, R. G. Hadt and D. G. Nocera, Organometallics, 2015, 34, 4766.
- 14 S. J. Hwang, D. C. Powers, A. G. Maher, B. L. Anderson, R. G. Hadt, S.-L. Zheng, Y.-S. Chen and D. G. Nocera, J. Am. Chem. Soc., 2015,
- 15 P. T. Matsunaga, G. L. Hillhouse and A. L. Rheingold, J. Am. Chem. Soc., 1993, 115, 2075.
- 16 R. Y. Han and G. L. Hillhouse, J. Am. Chem. Soc., 1997, 119, 8135.
- 17 K. Koo and G. L. Hillhouse, Organometallics, 1995, 14, 4421.
- 18 K. M. Koo, G. L. Hillhouse and A. L. Rheingold, Organometallics, 1995, 14, 456.
- 19 D. C. Powers, B. L. Anderson and D. G. Nocera, J. Am. Chem. Soc., 2013, 135, 18876.
- 20 R. Fayad, S. Engl, E. O. Danilov, C. E. Hauke, O. Reiser and F. N. Castellano, J. Phys. Chem. Lett., 2020, 11, 5345.
- 21 B. J. Shields and A. G. Doyle, J. Am. Chem. Soc., 2016, 138, 12719.
- 22 L. K. G. Ackerman, J. I. Martinez Alvarado and A. G. Doyle, J. Am. Chem. Soc., 2018, 140, 14059.
- 23 S. K. Kariofillis and A. G. Doyle, Acc. Chem. Res., 2021, 54, 988.
- 24 D. R. Heitz, J. C. Tellis and G. A. Molander, J. Am. Chem. Soc., 2016, 138, 12715.
- 25 B. Zheng, F. Z. Tang, J. Luo, J. W. Schultz, N. P. Rath and L. M. Mirica, J. Am. Chem. Soc., 2014, 136, 6499.
- 26 F. Z. Tang, N. P. Rath and L. M. Mirica, Chem. Commun., 2015,
- 27 W. Zhou, S. A. Zheng, J. W. Schultz, N. P. Rath and L. M. Mirica, J. Am. Chem. Soc., 2016, 138, 5777.
- 28 J. W. Schultz, K. Fuchigami, B. Zheng, N. P. Rath and L. M. Mirica, J. Am. Chem. Soc., 2016, 138, 12928.
- 29 M. B. Watson, N. P. Rath and L. M. Mirica, J. Am. Chem. Soc., 2017, **139**, 35,
- 30 P. Mondal, P. Pirovano, A. Das, E. R. Farquhar and A. R. McDonald, J. Am. Chem. Soc., 2018, 140, 1834.
- 31 J. B. Diccianni, C. H. Hu and T. N. Diao, Angew. Chem., Int. Ed., 2016, **55**, 7534.
- 32 R.-J. Cheng, C.-H. Ting, T.-C. Chao, T.-H. Tseng and P. P. Y. Chen, Chem. Commun., 2014, 50, 14265.
- 33 N. Kuwamura, K. i. Kitano, M. Hirotsu, T. Nishioka, Y. Teki, R. Santo, A. Ichimura, H. Hashimoto, L. J. Wright and I. Kinoshita, Chem. – Eur. J., 2011, 17, 10708.
- 34 K. A. Kozhanov, M. P. Bubnov, V. K. Cherkasov, G. K. Fukin, N. N. Vavilina, L. Y. Efremova and G. A. Abakumov, J. Magn. Reson., 2009, 197, 36.
- 35 W. Zhou, N. P. Rath and L. M. Mirica, Dalton Trans., 2016, 45, 8693.
- 36 D. M. Grove, G. van Koten, R. Zoet, N. W. Murrall and A. J. Welch, J. Am. Chem. Soc., 1983, 105, 1379.
- 37 A. W. Kleij, R. A. Gossage, R. J. M. Klein Gebbink, N. Brinkmann, E. J. Reijerse, U. Kragl, M. Lutz, A. L. Spek and G. van Koten, J. Am. Chem. Soc., 2000, 122, 12112.
- 38 B. Mougang-Soumé, F. Belanger-Gariépy and D. Zargarian, Organometallics, 2014, 33, 5990.
- 39 J.-P. Cloutier and D. Zargarian, Organometallics, 2018, 37, 1446.
- 40 J. R. Khusnutdinova, J. Luo, N. P. Rath and L. M. Mirica, Inorg. Chem., 2013, 52, 3920.
- 41 D. F. Evans, J. Chem. Soc., 1959, 2003.
- 42 J. Loliger and R. Scheffold, J. Chem. Educ., 1972, 49, 646.
- 43 D. M. Grove, G. Van Koten, P. Mul, A. A. H. Van der Zeijden, J. Terheijden, M. C. Zoutberg and C. H. Stam, Organometallics, 1986, 5, 322.
- 44 D. M. Grove, G. Van Koten, P. Mul, R. Zoet, J. G. M. Van der Linden, J. Legters, J. E. J. Schmitz, N. W. Murrall and A. J. Welch, Inorg. Chem., 1988, 27, 2466.
- 45 L. A. van de Kuil, Y. S. J. Veldhuizen, D. M. Grove, J. W. Zwikker, L. W. Jenneskens, W. Drenth, W. J. J. Smeets, A. L. Spek and G. van Koten, J. Organomet. Chem., 1995, 488, 191.
- 46 V. M. Iluc, A. J. M. Miller, J. S. Anderson, M. J. Monreal, M. P. Mehn and G. L. Hillhouse, J. Am. Chem. Soc., 2011, 133, 13055.
- 47 See ESI† for details.
- 48 R. L. Martin, J. Chem. Phys., 2003, 118, 4775.
- 49 Y. Kotake and K. Kuwata, Bull. Chem. Soc. Jpn., 1981, 54, 394.
- 50 G. R. Buettner, Free Radical Biol. Med., 1987, 3, 259.